Air Quality, Atmosphere & Health (2021) 14:1325–1339
https://doi.org/10.1007/s11869-021-01022-w

Polycyclic aromatic hydrocarbons in atmospheric particulate matter (PM_{10}) at a Southwestern Europe coastal city: status, sources and health risk assessment

Joel Sánchez-Piñero[1] · Jorge Moreda-Piñeiro[1] · Isabel Turnes-Carou[1] · María Fernández-Amado[1] · Soledad Muniategui-Lorenzo[1] · Purificación López-Mahía[1]

Received: 4 November 2020 / Accepted: 31 March 2021 / Published online: 8 April 2021

Abstract

Polycyclic aromatic hydrocarbons (PAHs) were assessed in 65 atmospheric particulate matter (PM_{10}) samples collected at a coastal urban area of Southwest Atlantic Europe during the 1-year period. Analytical methodology was successfully validated in terms of limits of detection and quantification, linearity, precision and trueness by using ERM CZ100 reference material and analytical recovery studies. Status of PM_{10}-bound PAHs and their relationship with other PM_{10} constituents (major ions, trace metals, equivalent black carbon (eBC) and UV-absorbing particulate matter (UVPM)) in an area where few data are available is provided. Benzo(b)fluoranthene (BbF) and benzo(e)pyrene (BeP) were observed to be predominant in all samples analysed with average concentrations of 1.6 and 1.5 ng m^{-3}, respectively. Furthermore, high RSDs were achieved for PAHs during the sampling period, which reflects inherent heterogeneity of the atmospheric particles besides weather conditions variations. Statistical significant seasonal changes in PAH concentrations during summer and winter seasons were not found. Data obtained from molecular PAH indices, univariate analysis, principal component analysis (PCA) and cluster analysis (CA) suggested a pyrogenic origin derived from the continuous harbour activity and marine and road traffic emissions at the studied urban site throughout the year. Additionally, major ion and metal(oid) concentrations in PM_{10} samples were also used as tracers of PAH origin and for PM_{10} source exploration. Linear and quadratic models have shown that the PAH concentrations exhibited correlation with some metals (Ba, Bi, Cu, Pb, Sb and Zn) and NO_3^- concentrations. Finally, carcinogenic and mutagenic potencies and inhalation cancer risk ($ILCR_{inh}$) posed by PM_{10}-bound PAHs were assessed.

Keywords Polycyclic aromatic hydrocarbons · Atmospheric particulate matter · Source contributions · Atlantic coastal European region · Health risk assessment

Introduction

Atmospheric particulate matter (PM) is a portion of air pollution that was classified by the International Agency for Research on Cancer (IARC) as carcinogenic to humans due to their harmful effects, representing a threat for human health (IARC 2013). Several epidemiological studies have associated the atmospheric PM exposure with an increase of morbidity and mortality due to respiratory and cardiovascular diseases (Taioli et al. 2007; Brook et al. 2010; Anderson et al. 2012; Hoek et al. 2013; Quarato et al. 2017; Burnett et al. 2018; Simonetti et al. 2018; Tobías et al. 2018; Muñoz et al. 2019). PM encompasses many associated pollutants which are potential contributors to adverse health effects after their entry into the organism through inhalation (Galvão et al. 2018). Among the pollutants that may either induce or increase PM toxicity, polycyclic aromatic hydrocarbons (PAHs) are notable because they constitute a large and diverse class of organic molecules that are widespread in the environment. In the atmosphere, PAHs are found in gas (lower molecular weight PAHs, i.e. 2- and 3-ring molecules) and particulate (medium-high molecular weight PAHs, i.e. 4-, 5- and 6-ring molecules) phases, depending on atmospheric conditions and vapour pressures of the compounds (Dat and Chang 2017). PAH sorption onto fine respirable particulate phase facilitates the

✉ Jorge Moreda-Piñeiro
jorge.moreda@udc.es

[1] Grupo Química Analítica Aplicada (QANAP), Instituto Universitario de Medio Ambiente (IUMA), Centro de Investigaciones Científicas Avanzadas (CICA), Department of Chemistry, Faculty of Sciences, University of A Coruña, Campus de A Coruña, s/n, 15071 A Coruña, Spain

transport of PAH over long distances and contributes to increase the adverse health effects of PAHs compounds, which can penetrate deep into the bronchioles and alveoli of the lungs. PAHs are mainly formed as a result of incomplete combustion or pyrolysis of organic matter such as fossil fuel burning (motor vehicle emissions, industrial fumes, domestic heating), incineration of organic waste and coal and biomass burning, whereas natural emissions include forest fires, volcanic eruptions and hydrothermal processes (Gozzi et al. 2017). The occurrence of PAHs in the environment is an increasing concern because of their potential persistence, bioaccumulation and carcinogenic, mutagenic and endocrine disrupting effects in human health (Kim et al. 2013; Karimi et al. 2015; Abdel-Shafy and Mansour 2016). Special interest and attention have been paid to 16 PAHs designated as priority pollutants by United States Environmental Protection Agency (USEPA) (USEPA 1984). Among these priority PAHs, benzo(a)pyrene (BaP) is used as a marker for carcinogenic/mutagenic health risk assessment due to its being considered to exhibit the most adverse effect. In addition, BaP is the only PAH subjected to regulatory guidelines in PM, setting a value of 1 ng m^{-3} (annual mean concentration) in PM_{10} fraction (mean particulate matter which passes through a size-selective inlet with a 50% efficiency cut-off at 10-μm aerodynamic diameters) by the European Union (EU), seeking to avoid adverse effects of PAHs to health and the environment (EU 2004).

In the last decades and due to their carcinogenic/mutagenic properties, PAH concentrations have been closely monitored at urban, rural and industrial atmospheres around the world to assess human exposure to PAHs. However, only few studies have been focused at Southwest Atlantic European Coast sites (Arruti et al. 2012; Slezakova et al. 2013a, b; Albuquerque et al. 2016; Alves et al. 2016; Elorduy et al. 2016; Cerqueira and Matos 2019). Concentrations, possible emission sources and associated health risks of particulate PAHs in urban atmospheres of Lisbon (Cerqueira and Matos 2019), Porto (Slezakova et al. 2013a, b; Albuquerque et al. 2016) and Braga cities (Alves et al. 2016) in Portugal have been reported. Also, some data can be also found at two Atlantic cities of Spain: Bilbao city, northern Spain (Elorduy et al. 2016), urban cities (Santander, Castro Urdiales and Reinosa) and rural areas (Los Tojos) in the region of Cantabria (Arruti et al. 2012). This paper aims to provide information of seasonal variation, sources and carcinogenic/mutagenic risks of PM_{10}-associated PAHs at the Southwest Atlantic facade of Europe, where few data are available. Furthermore, the relationship between PM_{10}-bound PAHs and PM_{10} components such as major ions, metal(oid)s, equivalent black carbon (eBC) and UV-absorbing particulate matter (UVPM) was also investigated.

Materials and methods

Details and description of the study area

The sampling site is located at 5 m above sea level inside the downtown of the city of A Coruña (43° 22′ 04″ N 08° 25′ 08″ W), an Atlantic coastal city with a quarter of a million inhabitants in the northwest of Spain which occupies a small peninsula (Fig. 1). The climate of the city is humid oceanic characterized by moderate temperatures, constant relative humidity and frequent rainfalls throughout the year (especially during winter). Then, two seasons could be considered in the present study attending to meteorological similarities: summer (warm season: April–September) and winter (cold season: October–March). Several anthropogenic sources (Fig. 1) are accounted due to the proximity of several industrial areas near the city (aluminium processing, refinery, power plants, and municipal solid waste and biomass incinerators). Moreover, emissions from maritime and road traffic could be important anthropogenic sources. Due to the sea proximity, marine aerosol influence is also important and sea salt presence is significant.

Atmospheric particulate matter sample collection

Sampling and PM_{10} determination were according to the European Norm 12341 (EN 12341:2015) (UNE 2015). Samplings were performed during January to December 2017 using an automatic high-volume sampler DIGITEL DHA-80 (Hegnau, Switzerland) provided with a 10-μm diameter cut-off particle separator and pre-heated micro quartz fibre filters of 15 cm of diameter (Ahlstrom Munksjö MK 360, Falun, Sweden). Atmospheric particulate matter was collected at 30 m^3 h^{-1} for 24 h, 0 to 24 h (UTC). Before and after sampling, filters were stabilized at 20 ± 1 °C and relative humidity of 45–50% for 48 h, for mass weighing by means of an analytical balance (Sartorius Genius, Goettingen, Germany) with a sensitivity of 0.01 mg. Once the gravimetric determination of PM_{10} was performed, PM_{10} filters were folded and wrapped in aluminium foils inside envelopes, put inside sealed plastic bags and stored in the lab in a freezer (−18 °C) until analysis to avoid the losses of volatile compounds, especially during summer season. A total of 65 samples were selected covering all the months of the campaign (one/two randomized samples at week, distributed over the year). Samples collected are in agreement with minimum sample number for indicative measurements, according to European Directive 2008/50/EC (EU 2008). Additionally, field blanks were also collected to decrease gravimetric bias due to filter handling during and/or after sampling, which were analysed following the same procedure as samples (procedure blanks).

Fig. 1 Sampling point situation in A Coruña city (Spain). Source: Google Maps (satellite maps, without annotations) and Mapchart.net (https://mapchart.net/spain.html)

PAH extraction procedure and quantification by HPLC-FLD

PAH content in PM_{10} samples was assessed following the method described by Piñeiro-Iglesias (Piñeiro-Iglesias et al. 2003, 2004) with some modifications. Briefly, four circular portions of each PM_{10} sample (area of 5.31 cm^2) were cut and extracted by using hexane:acetone 1:1 assisted with microwave energy (ETHOS SEL microwave system, Milestone, Sorisole, BG, Italy). Extracts were cleaned up (Supelclean™ LC-Si SPE Tubes (Supelco, Steinheim, Germany)), concentrated (TurboVap® II Concentration Workstation (Biotage, Uppsala, Sweden)) and then to dryness using a gentle stream of N_2. Extracts were reconstituted by using 500 μL of acetonitrile for subsequent analysis. PAHs were determined in PM_{10} extracts by using a chromatographic system (Waters, Milford, MA, USA) equipped with programmable fluorescence detector (Waters 2475) and a Waters® PAH C18 (250 × 4.6 mm i.d., 5 μm) column. A chromatographic separation and fluorescence conditions were performed basing on the work of Fernández-Amado et al. (Fernández-Amado et al. 2016). In supporting Information (SFigure 1) shows a chromatogram obtained for a mixture of target PAHs at 25 μg L^{-1} HPLC-FLD conditions used in this study. Moreover, details of quality assurance and control of PAH extraction and quantification procedures are also shown in Supporting Information.

Exposure assessment and health risk assessment

The carcinogenicity of environmental exposure to PM_{10}-associated PAHs relatively to BaP equivalent (BaP_{Teq}) concentration of 16 PAHs ($\Sigma_{16}BaP_{Teq}$) was calculated using the following formula (Gao et al. 2019):

$$\sum_{16}\left[\mathrm{BaP_{Teq}}\right] = \sum_{i=1}^{i=16}\left([\mathrm{PAH}_i]\ x\ \mathrm{TEF}_i\right)$$

where $[PAH_i]$ represents the concentration of each PAH in PM_{10} samples (expressed as ng m^{-3}), and TEF_i is the toxic equivalence factor of the PAH_i relative to BaP. TEFs used in this study were 0.001 for naphthalene (Naph), acenaphthene (Ace), fluorene (Fl), phenanthrene (Phe), fluoranthene (Ft) and pyrene (Pyr); 0.01 for anthracene (Ant), chrysene (Chry) and benzo(g,h,i)perylene (BghiP); 0.1 for benzo(a)anthracene (BaA), benzo(b)fluoranthene (BbF), benzo(k)fluoranthene (BkF) and indeno(1,2,3-cd)pyrene (IP); 1.0 for benzo(e)pyrene (BeP) and BaP; and 5.0 for dibenz(a,h)anthracene (DBahA) (Samburova et al. 2017).

Similarly, the total mutagenicity of PM_{10}-associated PAHs relatively to BaP mutagenic equivalent (BaP_{Meq}) concentration of 8 USEPA priority PAHs (Σ_8BaP_{Meq}) was calculated using the following formula (Durant et al. 1996):

$$\sum_{8}\left[\mathrm{BaP_{Meq}}\right] = \sum_{i=1}^{i=8}\left([\mathrm{PAH}_i]\ x\ \mathrm{MEF}_i\right)$$

where MEF_i is the mutagenic equivalence factor (MEF) value of the PAH_i. MEFs used in this study were 0.082, 0.017, 0.25, 0.11, 1, 0.29, 0.19 and 0.31, for BaA, Chry, BbF, BkF, BaP, DBahA, BghiP and IP, respectively (Durant et al. 1996).

Incremental lifetime cancer risk refers to the probability of an individual who is exposed to PM_{10}-associated PAHs by inhalation during his or her lifetime were also estimated (USEPA 2005; WHO 2010). The $ILCR_{inh}$ values were calculated using the following formula:

$$\mathrm{ILCR_{inh}} = \mathrm{IUR_{BaP}}\ x\ \sum_{16}\left[\mathrm{BaP_{Teq}}\right]$$

where $ILCR_{inh}$ is the incremental lifetime cancer risks resulting from the PM_{10} inhalation pathway and IUR_{BaP} is the inhalation unit cancer risk factor (expressed as ng $m^{-3})^{-1}$ for BaP. IUR_{BaP} describes the theoretical upper limit possibility of contracting cancer calculated for a daily exposure to BaP concentration in air of 1.0 μg m^{-3} for a 70-year average life span (OEHHA 2005; USEPA 2011). Quantitative cancer risk estimates of PAHs as air pollutants are very uncertain because of the lack of useful and good-quality data and due to an estimated IUR_{BaP} based on epidemiology studies of populations from A Coruña is not available, several international accepted values for estimated IUR_{BaP}, based on different

approaches (epidemiology study on coke-oven workers in Pennsylvania, $IUR_{BaP} = 8.7 \times 10^{-5}$ (ng $m^{-3})^{-1}$ (WHO 2000); and studies on the data respiratory tract tumours in hamsters chronically exposed by inhalation to BaP, 1.1×10^{-6} (ng $m^{-3})^{-1}$ (OEHHA 2005) and 6.0×10^{-7} (ng $m^{-3})^{-1}$ (USEPA 2017)) were used in this work to calculate the PM_{10}-bound PAH $ILCR_{inh}$. When $ILCR_{inh} \leq 10^{-6}$ denotes negligible or virtual safety under most regarding regulatory programmes, $ILCR_{inh}$ among 10^{-6} and 10^{-4} suggests a potential risk and $ILCR_{inh} > 10^{-4}$ imply potentially high risk (Wang et al. 2011; Cao et al. 2019; Ghanavati et al. 2019).

Additional data

Major ion and trace metal(oid) quantification

Major ions in PM_{10} samples were measured by zone capillary electrophoresis (ZCE) after aqueous extraction and metal(oid)s were measured by inductively coupled plasma mass spectrometry (ICP-MS) after acid extraction. Both procedures were previously optimized (Blanco-Heras et al. 2008; Moreda-Piñeiro et al. 2015). Statistical summary for the concentrations of major ions and metals in 65 PM_{10} samples are shown in STable 1–2.

Equivalent black carbon and UV-absorbing particulate matter quantification

eBC and UVPM were measured by using a Magee SootScan™ OT-21 (Berkeley, CA, USA) transmissometer at two wavelengths: measurements at 880 nm are interpreted as a measure of light-absorbing carbon analogous to black carbon present on the filter, while measurements at 370 nm are designated as UVPM indicator of aromatic organic compounds (Davy et al. 2017; Greilinger et al. 2019). Results obtained in PM_{10} samples are shown in STable 1.

Backward trajectory analysis

Backward trajectories were calculated at 2500, 1500 and 750 m above mean sea level (AMSL) 120 h before the time of the arrival to study site using the NOAA Hybrid Single-Particle Lagrangian Integrated Trajectory Model (HYSPLIT) model (Draxler and Rolph 2003).

Statistical treatment of data

For analytical data treatment, the ANOVA test was performed in order to verify the statistical significance of the differences between the means assessment; Pearson coefficients were calculated in order to investigate the existence of possible associations; principal component analysis (PCA) and cluster analysis (CA) were performed in order to identify the PAHs emission sources in the study area; and multivariate analysis based on quadratic surface model was performed to assess statistically significant relationship between variables. All statistical procedures were performed using the statistical package Statgraphics version 7.0 routine (Statgraphics Graphics Corporation, ST.SC., USA) at the 95% confidence level. In this study, PCA analysis was performed, after half-range and central value transformation, by utilising the orthogonal transformation method with Varimax rotation and retention of principal components which show eigenvalues higher than 1.0. Finally, CA was performed after half-range and central value transformation, using Ward's clustering method and squared Euclidian distance metric. When PAH concentrations were below the quantification limits, values were approximated to LOQs/2 for statistical calculations. All PAHs, except for Naph, were used to estimate total PAHs bound to PM_{10} (Σ_{15}PAH i.e. the sum of concentrations of individual species) assessment. However, Naph, Ace, Fl and Ant were not included in univariate, multivariate, cluster and PCA analyses because of having found concentrations below LOQs for the majority of PM_{10} samples.

Results and discussion

PM_{10} mass concentrations

According to the gravimetric measurements, average PM_{10} mass concentrations during the whole period were 23.5 μg m^{-3} (Table 1). The highest PM_{10} mass concentration was measured for one sample (94 μg m^{-3}) during the winter season (on 15 October 2017), which exceeds the daily limit value of 50 μg m^{-3} set in the European Directive 2008/50/EC (EU 2008). This was the only daily exceedance observed in analysed samples, which cannot be exceeded more than 35 times per year (EU 2008). The Saharan dust incursion during 12 to 17 October 2017 at the sampling site could explain the PM_{10} mass concentration of 94 μg m^{-3} during 15 October 2017 (see Backward Trajectory Analysis, SFigure 2). Despite, the average PM_{10} mass concentration during the winter season corresponds with 25.7 μg m^{-3}. Also, PM_{10} concentrations in summer and winter seasons showed no statistically significant differences (the *p*-value of the *F*-test is higher than 0.05) at 95.0% confidence level (STable 3).

Atmospheric particle-bound PAH concentrations in PM_{10}

Summary data of PAHs concentrations (mean, maximum, minimum and RSD) in PM_{10} samples during the whole sampling period studied and during summer and winter seasons are reported in Table 1. BbF and BeP were predominant PAHs in all samples collected with average concentrations of 1.6 and

Table 1 Average, maximum (max), minimum (min) and RSD (%) values of PM_{10} mass (μg m^{-3}), individual PM_{10}-bound PAHs and PAH summations (of 15 PAHs (Σ_{15}PAHs), carcinogenic PAHs (ΣPAHc), non-carcinogenic PAHs (ΣPAHnc), 4 rings PAHs ΣPAH_{4rings} and 5–6 rings PAHs $\Sigma PAH_{5-6rings}$) concentrations (ng m^{-3})

	Average	Max	Min	RSD
Whole period (*N*=65)				
PM_{10} mass	23.5	94.0	10.0	50
Ace	0.080	2.3	<0.022	363
Fl	0.015	0.27	<0.016	228
Phe	0.18	1.8	<0.099	161
Ant	0.009	0.23	<0.005	328
Ft	0.33	1.5	<0.057	113
Pyr	0.31	1.3	<0.083	144
BaA	0.25	1.5	<0.041	128
Chry	0.85	4.1	<0.15	114
BeP	1.5	7.5	<0.18	112
BbF	1.6	8.7	<0.20	111
BkF	0.44	2.1	<0.063	109
BaP	0.48	2.2	<0.046	113
DBahA	0.081	0.54	<0.022	129
BghiP	0.88	3.9	<0.10	100
IP	0.61	2.7	<0.073	101
Σ_{15}PAHs	7.7	33.4	0.58	96
ΣPAHc	4.4	19.7	0.30	108
ΣPAHnc	3.3	13.7	0.28	100
ΣPAH_{4rings}	1.7	7.4	0.16	109
$\Sigma PAH_{5-6rings}$	5.6	26.0	0.35	107
Summer season (*N*=32)				
PM_{10} mass	20.0	42.0	10.0	40
Ace	0.019	0.43	<0.022	386
Fl	0.016	0.27	<0.016	290
Phe	0.13	1.2	<0.099	198
Ant	0.004	0.23	<0.005	924
Ft	0.26	1.4	<0.057	138
Pyr	0.22	1.2	<0.083	134
BaA	0.27	0.70	<0.041	69
Chry	0.94	4.17	<0.15	102
BeP	1.7	7.5	<0.18	115
BbF	1.8	8.7	<0.20	121
BkF	0.45	2.1	<0.063	120
BaP	0.49	1.9	<0.046	99
DBahA	0.085	0.54	<0.022	150
BghiP	0.86	3.9	<0.10	113
IP	0.58	2.7	<0.073	118
Σ_{15}PAHs	7.8	33.4	0.58	110
ΣPAHc	4.6	19.7	0.30	111
ΣPAHnc	3.2	13.7	0.28	111
ΣPAH_{4rings}	1.7	7.4	0.16	101
$\Sigma PAH_{5-6rings}$	5.9	26.0	0.35	116
Winter season (*N*=33)				
PM_{10} mass	25.7	94.0	10.0	55
Ace	0.13	2.3	<0.022	298
Fl	0.013	0.089	<0.016	133
Phe	0.22	1.8	<0.099	143
Ant	0.007	0.038	<0.005	130
Ft	0.43	1.5	<0.057	88
Pyr	0.43	1.3	<0.083	134
BaA	0.38	1.5	<0.041	99
Chry	1.1	3.8	<0.15	87
BeP	1.7	5.8	<0.18	81
BbF	1.8	5.5	<0.20	80
BkF	0.53	1.5	<0.063	77
BaP	0.64	2.2	<0.046	87
DBahA	0.088	0.29	<0.022	90
BghiP	1.1	2.8	<0.10	70
IP	0.75	1.8	<0.073	70
Σ_{15}PAHs	9.3	27.4	0.68	75
ΣPAHc	5.3	16.2	0.33	79
ΣPAHnc	4.0	11.2	0.35	74
ΣPAH_{4rings}	2.3	7.0	0.16	84
$\Sigma PAH_{5-6rings}$	6.6	19.5	0.39	76

1.5 ng m^{-3}, respectively (Table 1). Other PAHs followed the sequence BghiP (0.88 ng m^{-3}) > Chry (0.85 ng m^{-3}) > IP (0.61 ng m^{-3}) > BaP (0.48 ng m^{-3}) > BkF (0.44 ng m^{-3}) > Ft (0.33 ng m^{-3}) > Pyr (0.31 ng m^{-3}) > BaA (0.25 ng m^{-3}) > Phe (0.18 ng m^{-3}) > DBahA (0.08 ng m^{-3}) ~ Ace (0.08 ng m^{-3}) > Fl (0.02 ng m^{-3}) and Ant (0.009 ng m^{-3}) (Table 1). Naph (most volatile PAH mainly present in the gas phase) were the least abundant with concentrations lower than LOQ in all PM_{10} samples. Other volatile PAHs (Ace, Fl and Ant) offer concentrations lower than their LOQs in almost all PM_{10} samples (mainly during warm months). Target PAHs demonstrated high variation from event to event (Table 1), which reflect inherent heterogeneity of the atmospheric particles (PM_{10} sources) and the variability of meteorological conditions.

Despite differences in the number of target PAHs measured and sampling period times, the sum of PAH concentrations (Σ_{15}PAHs) achieved in this study was compared with ΣPAH values reported in PM_{10} samples from other urban sites collected at Southwest Atlantic European Coast. The annual range (0.58 to 33.4 ng m^{-3}, Table 1) is higher than those found in Lisbon (Portugal), 0.11 to 8.2 ng m^{-3} range (for Σ_{10}PAHs) (Cerqueira and Matos 2019) and Bilbao (Spain), 1.2 to 9.8 ng m^{-3} range (diurnal range, sampling period of 8 h, for Σ_{13}PAHs) (Elorduy et al. 2016) and lower than reported in Oporto (Portugal), from 30.8 (annual mean during 2014) to

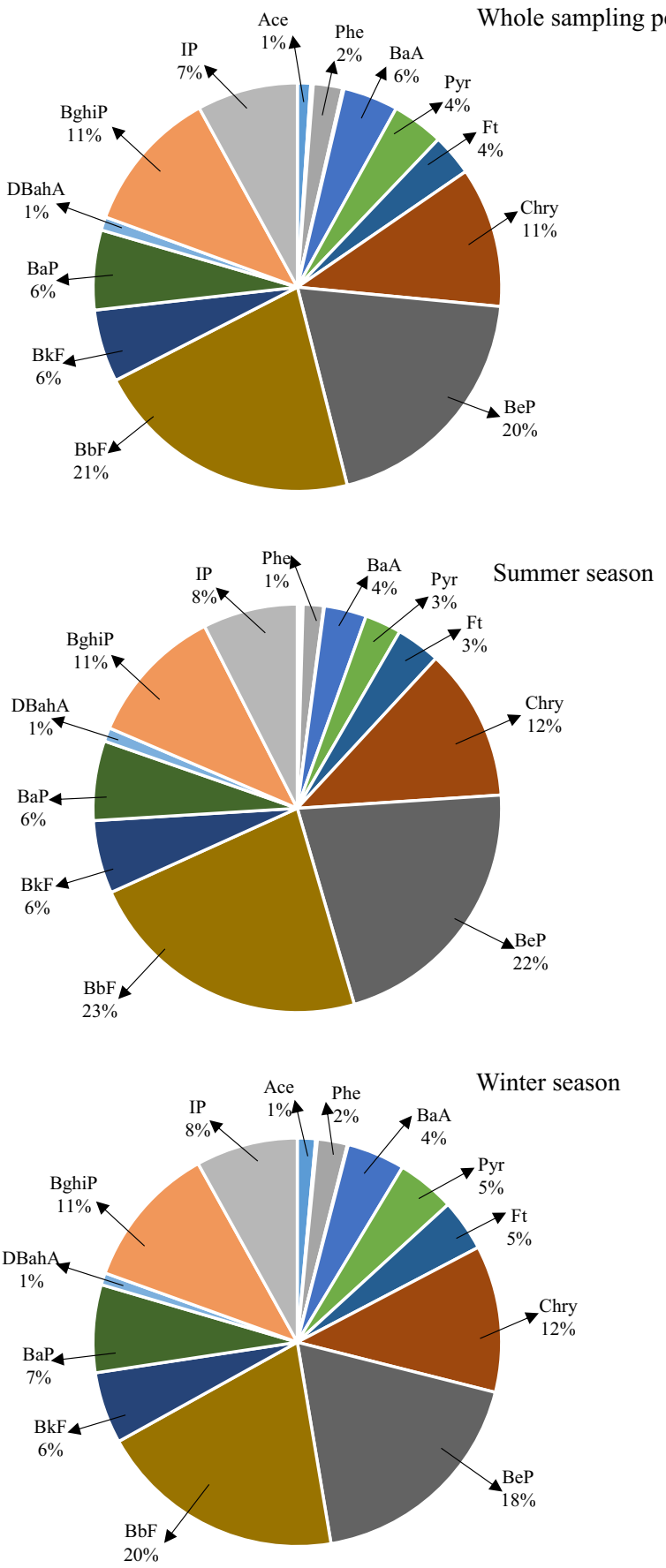

Fig. 2 Compositions in percentages of PAHs during 1-year sampling and summer and winter seasons

126.5 (annual mean during 2004) ng m^{-3} (for Σ_{10}PAHs) (Albuquerque et al. 2016) and 16.8 to 149 ng m^{-3} range, with a mean of 70 ng m^{-3} range (for Σ_{18}PAHs in air, i.e. sum of concentrations of all PAHs both in gas phase and in PM_{10} particles) (Slezakova et al. 2013a, b).

Furthermore, the average annual concentration of BaP (0.48 ng m^{-3}) was significantly lower than the annual value set in 1.0 ng m^{-3} by the European Directive (EU 2004). However, this limit was exceeded by 9 samples during the studied period (2 and 7 samples during summer and winter seasons, respectively). However, the average BaP concentration is higher than previous reported data, i.e. <LOD to 0.85 ng m^{-3} (Cerqueira and Matos 2019), 0.15 to 0.94 ng m^{-3} (Albuquerque et al. 2016), 0.06 to 0.70 ng m^{-3} (Elorduy et al. 2016) and 0.04 to 0.15 ng m^{-3} (Arruti et al. 2012) in PM_{10} samples collected at several Southwest Atlantic European cities (Lisbon (Cerqueira and Matos 2019), Oporto (Albuquerque et al. 2016), Bilbao (Elorduy et al. 2016) and Santander and Reinosa cities (Arruti et al. 2012) respectively).

Higher mean PAH concentrations were obtained during the winter than summer season. However, after applying ANOVA (STable 3), statistically significant differences (at 95.0% confidence level) between summer and winter seasons were not found (p-value > 0.05). The continuous harbour activity, as well as maritime and road traffic in the area, might explain the occurrence of PM_{10}-bound PAHs throughout the year, with no differences between seasons.

BbF and BeP amounted to 41, 45 and 38% of the total PAHs bound to PM_{10} (Σ_{15}PAH i.e. the sum of concentrations of individual species) during the whole sampling period and during summer and winter seasons, respectively (Fig. 2). In Fig. 2 is also shown the relative percentage contributions of other priority PAHs (which contribution is less than 1%) during the whole sampling period and during summer and winter times.

The carcinogenic PAHs (BbF, Chry, IP, BaP, BkF, BaA and DBahA) concentrations (Σ_cPAH) and non-carcinogenic PAHs (Ace, Fl, Phe, Ant, Ft, Pyr, BeP, BghiP) concentrations (Σ_{nc}PAH) represented 58–60% and 40–42% of PAHs, respectively. The distribution of carcinogenic and non-carcinogenic PAHs in PM_{10} was similar for both seasons. BbF was the most abundant carcinogenic PAH, representing 21, 23 and 20% of PAH in mean during a year, summer season and winter season, respectively.

Distribution of PAHs on molecular weight basis shown that lower ring-number molecules, 2–3 rings, $\Sigma_{2-3rings}$PAH, (Ace, Fl, Phe and Ant) are partitioned mainly into the gas phase; thus, $\Sigma_{2-3rings}$PAH accounted for only 2–4%. Middle ring-number molecules, (Σ_{4rings}PAH), (Ft, Pyr, BaA and Chry) accounted for 37–44%, while high ring-number molecules, ($\Sigma_{5-6rings}$PAH), (BeP, BbF, BkF, BaP, IP, DBahA, BghiP) accounted for 71–76% (Fig. 2). The distribution of low, middle and high ring-number molecules was constant in the two seasons. Also, the high proportions of high ring-number molecules and the good correlation between Σ_{15}PAH and BghiP content during the whole sampling period (R^2=0.9771) and both seasons (R^2=0.9817 and 0.9701 for summer and winter seasons, respectively) (SFigure 3) indicate that high-temperature processes such as combustion of fuels derived from harbour activities as well as road and ship traffic could be the main sources of particulate PAHs at sampling site.

Source apportionment of PAHs

A study about the association between particle-bound PAH concentrations and PAH sources was assessed. Molecular

Table 2 Values (average ± SD[a]) estimated for diagnostic PAHs ratios and p-values achieved after statistical comparison of average PAH ratios during summer and winter seasons

	Whole period	Summer season	Winter season	p-value
Ft/Ft+Pyr ratio	0.51±0.10	0.55±0.11	0.50±0.10	0.059
BaA/(BaA+Chry) ratio	0.21±0.08	0.20±0.07	0.25±0.07	0.005
BaP/BghiP ratio	0.49±0.13	0.47±0.08	0.55±0.14	0.007
IP/(IP+BghiP) ratio	0.41±0.05	0.43±0.06	0.42±0.04	0.431
BaP/(BaP+Chry) ratio	0.34±0.09	0.32±0.09	0.37±0.09	0.029

Pyrogenic source: Ft/(Ft+Pyr) ratio >0.5 (Yunker et al. 2002)

Petrogenic source: Ft/(Ft+Pyr) and BaA/(BaA+Chry) ratios <0.5 and <0.2, respectively (Yunker et al. 2002)

Vehicle emissions: Ft/(Ft+Pyr) between 0.4 and 0.5 and BaP/BghiP ratio < 0.6 (Yunker et al. 2002; Jamhari et al. 2014)

Mixed sources: BaA/(BaA+Chry) ratio in the range of 0.2 to 0.35 (Yunker et al. 2002)

Fuel combustion source: BaA/(BaA+Chry) ratio > 0.35 and IP/(IP+BhijP) ratio <0.5 (Yunker et al. 2002; Vicente et al. 2018)

Biomass and coal combustion source: IP/(IP+BhijP) ratio >0.5 (Yunker et al. 2002; Vicente et al. 2018)

Diesel combustion: BaP/(BaP+Chry) ratio <0.5 (Teixeira et al. 2012)

Gasoline combustion: BaP/(BaP+Chry) ratio >0.5 (Teixeira et al. 2012)

[a] Standard deviation

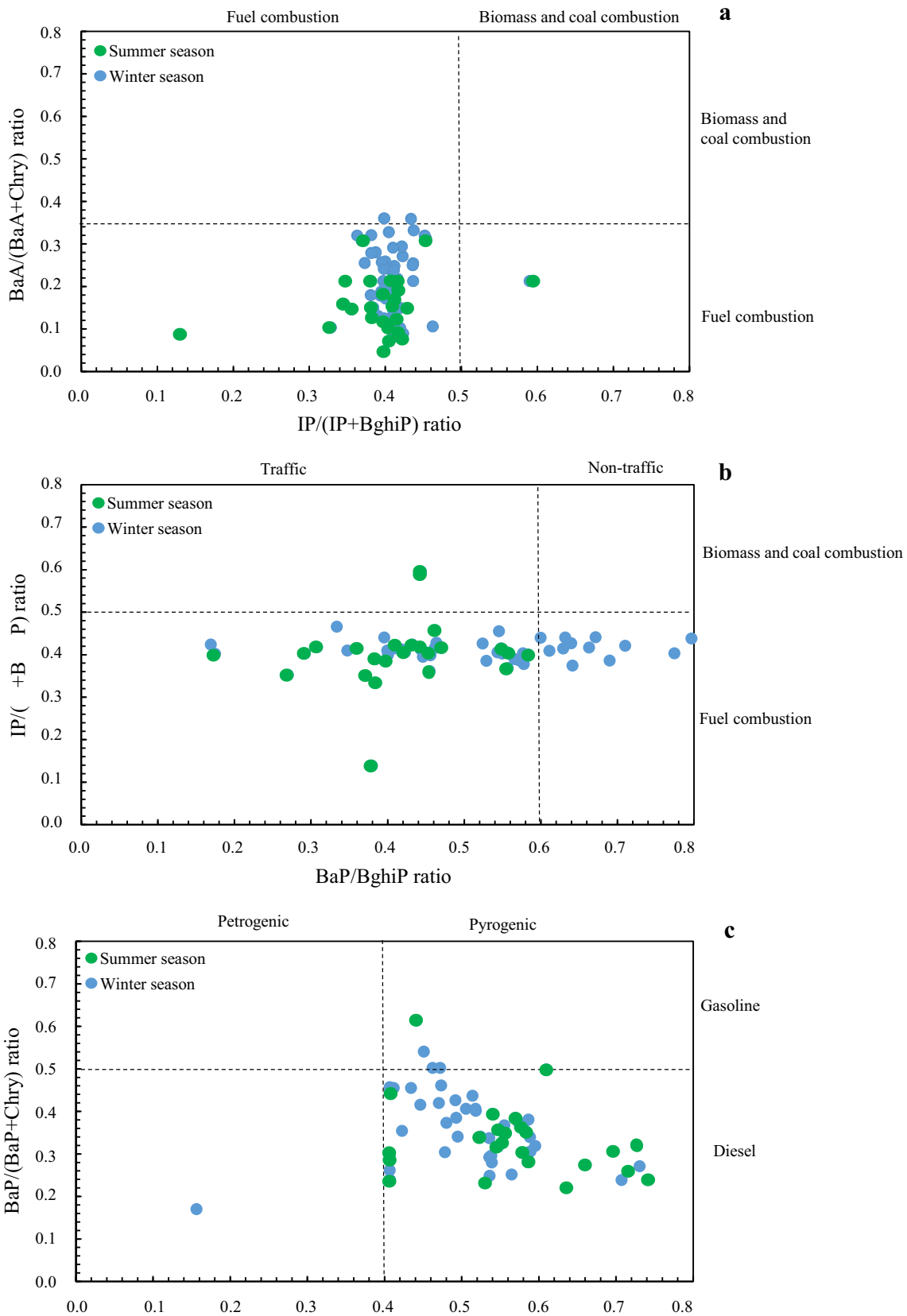

Fig. 3 Cross-plots for selected PAHs diagnostic ratios: **a** BaA/(BaA+Chry) ratio vs. IP/(IP+BghiP) ratio. **b** IP/(IP+BghiP) ratio vs. BaP/BghiP ratio. **c** BaP/(BaP+Chry) ratio vs. Ft/(Ft+Pyr) ratio

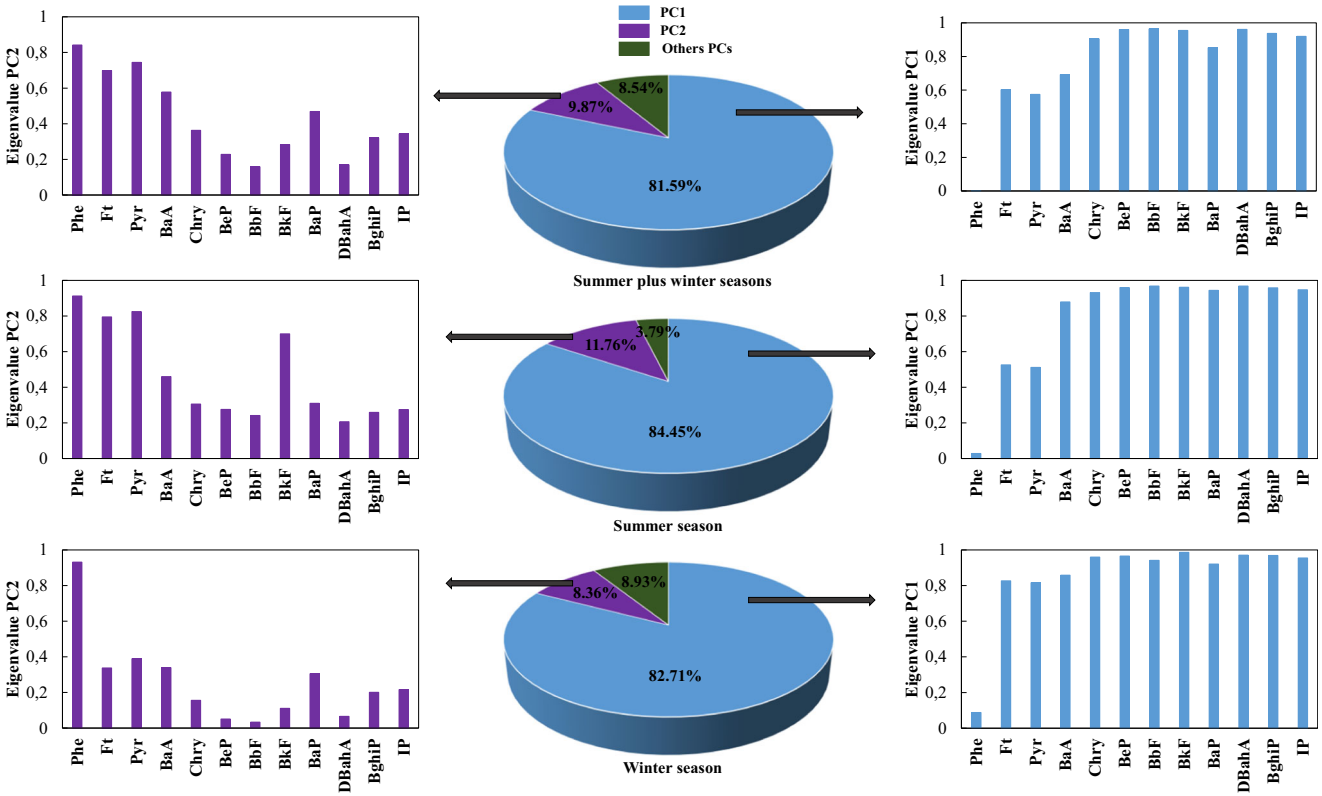

Fig. 4 Proportion of variance contributions in percentage from PCA analysis for Phe, Ft, Pyr, BaA, Chry, BeP, BbF, BkF, BaP, DBahA, BghiP and IP concentrations in PM_{10} samples collected during the whole period (N=65) and summer (N=32) and winter (N=33) seasons

indices (PAH ratios) and the relationship between PAH concentrations and the contents of major ions, metal(oid)s, eBC and UVPM in PM_{10} samples were studied by univariate and multivariate analyses, principal component analysis (PCA) and cluster analysis (CA).

Molecular indices

Molecular indices based on PAH physical-chemical behaviour covariability were usually used as diagnostic ratios to identify and estimate the contribution of main PAHs sources: pyrogenic combustion (incomplete combustion of petroleum fuel and vehicular exhaust emission) and petrogenic sources (unburned crude oil and petroleum products) (Yunker et al. 2002). Nonetheless, the overlapping of different PAH sources and the transformation/decomposition of some PAH species due to their reactivity into the atmosphere make difficult the identification of potential emission sources of PAHs. Then, the analysis of more PAHs such as alkylated PAHs would provide a more reliable source identification.

Several commonly used diagnostic ratios, i.e. Ft/(Ft+Pyr), BaA/(BaA+Chry), BaP/BghiP, IP/(IP+BghiP) and BaP/(BaP+Chry) ratios were selected to distinguish the major source PAHs in the study area. Ft and Pyr are pyrogenic products derived from high-temperature condensation of lower molecular weight aromatic compounds, Ft being less thermodynamically stable than Pyr. The predominance of Ft over Pyr is characteristic of a pyrogenic process, while in petroleum-derived PAHs, Pyr is more abundant than Ft. A ratio of Ft/(Ft+Pyr) > 0.5 suggests emissions from coal and biomass burning, Ft/(Ft+Pyr) < 0.4 petrogenic sources, while Ft/(Ft+Pyr) ratios between 0.4 and 0.5 would point out vehicle emissions (Yunker et al. 2002). Chry, BaA, BghiP and IP are derived from processes of organic matter combustion at high temperature. Thus, BaA/(BaA+Chry) ratio > 0.35 suggests combustion of fossil fuels, < 0.2 petrogenic sources (unburned fossil material) and the range between 0.2 and 0.35 would indicate the mixture of petroleum and combustion sources (Yunker et al. 2002). Also, the BaP/BghiP ratio is used to differentiate traffic and non-traffic sources, then BaP/BghiP < 0.6 would indicate vehicles emissions (Jamhari et al. 2014). The IP/(IP+BghiP) ratio is used to distinguish liquid fossil fuel combustion from biomass and coal combustion sources, IP/(IP+BghiP) ratios < 0.5 suggests fossil fuel combustion, while IP/(IP+BghiP) ratios > 0.5 suggests coal/biomass combustion sources (Yunker et al. 2002; Vicente et al. 2018). Finally, the BaP/(BaP+Chry) ratio was used to distinguish diesel combustion (< 0.5) and gasoline combustion (> 0.5) sources (Teixeira et al. 2012).

Despite the limitations of this approach and the fact that the averages of BaA/(BaA+Chry), BaP/BghiP and BaP/(BaP+Chry) ratios for the warm season were statistically significant

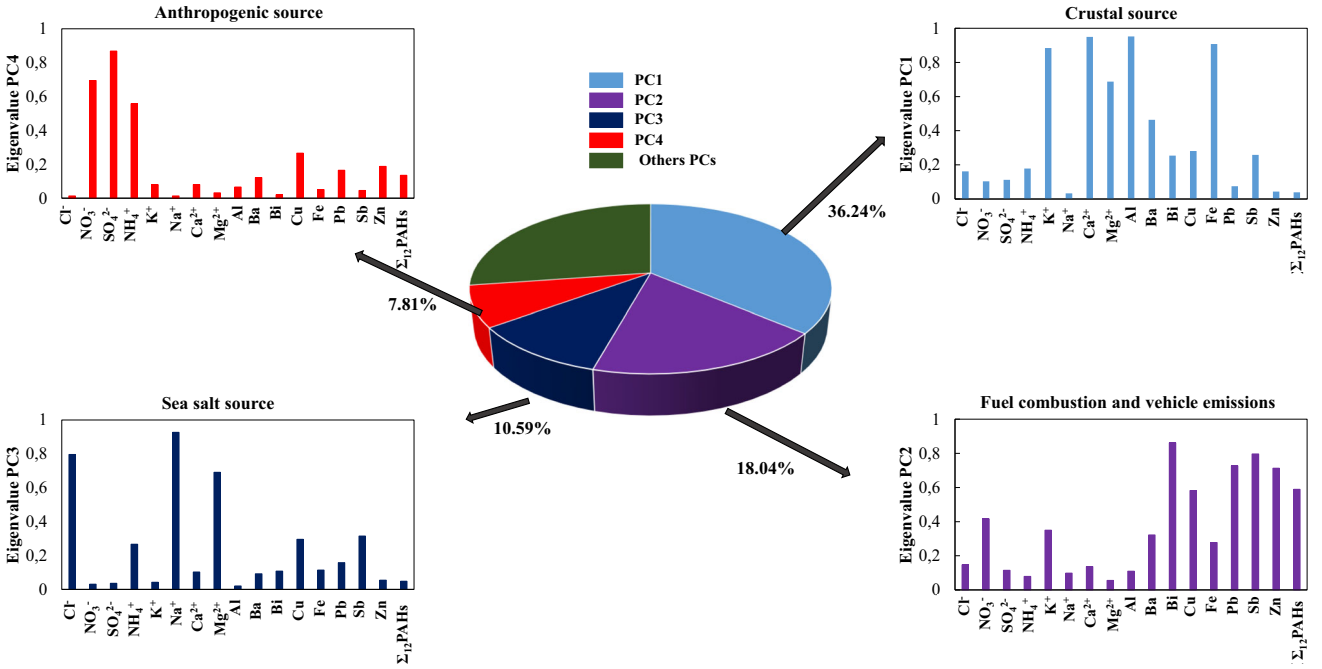

Fig. 5 Source composition and proportion of variance contributions in percentage from PCA analysis for PM_{10} samples collected during the study period (N=65). Σ_{12}PAH= Phe, Ft, Pyr, BaA, Chry, BeP, BbF, BkF, BaP, DBahA, BghiP and IP

different ($p < 0.05$) from that of the cold season (Table 2), Ft/(Ft+Pyr), BaA/(BaA+Chry) and IP/(IP+BghiP) ratios would suggest pyrogenic sources (incomplete fuel combustion) for PAHs during summer and winter periods (Table 2). BaA/(BaA+Chry), IP/(IP+BghiP) and BaP/BghiP ratios also suggested mixed sources, fuel combustion source and vehicle emissions during both seasons, respectively. Also, most of the samples shown a BaP/(BaP+Chry) ratio lower than 0.5, which suggests that PAH emissions from diesel combustion prevailed over gasoline combustion during total period (Table 2). Finally, in Fig. 3a, b is presented a plot of BaA/(BaA+Chry) versus IP/(IP+BghiP) ratios and IP/(IP+BghiP) versus BaP/BghiP ratios respectively, suggesting pyrogenic sources (fuel combustion) during both seasons. Furthermore, diesel combustion (most likely due to the harbour activities and vehicular emissions) was observed to be the predominant source of PAHs during both seasons when plotting BaP/(BaP+Chry) ratio versus Ft/(Ft+Pyr) ratio (Fig. 3c).

Univariate analysis

Pearson product moment correlations of Σ_{12}PAH, Σ_cPAH, Σ_{nc}PAH, Σ_{4rings}PAH and $\Sigma_{5-6rings}$PAH contents with major ions, metal(oid)s, eBC and UVPM (at a confidence level of 95%) were assessed for samples collected for 1 year long (STable 4). Results show that Σ_{12}PAH, Σ_cPAH, Σ_{nc}PAH, Σ_{4rings}PAH and $\Sigma_{5-6rings}$PAH contents are correlated with NO_3^-, As, Bi and Zn (anthropogenic sources, including fossil fuel combustion and road traffic). Finally, a positive correlation between eBC (p-value < 0.0002) and UVPM (p value < 0.0008) were found for Σ_{12}PAHs, Σ_cPAHs, Σ_{nc}PAHs, Σ_{4rings}PAHs and $\Sigma_{5-6rings}$PAHs. Moreover, a correlation

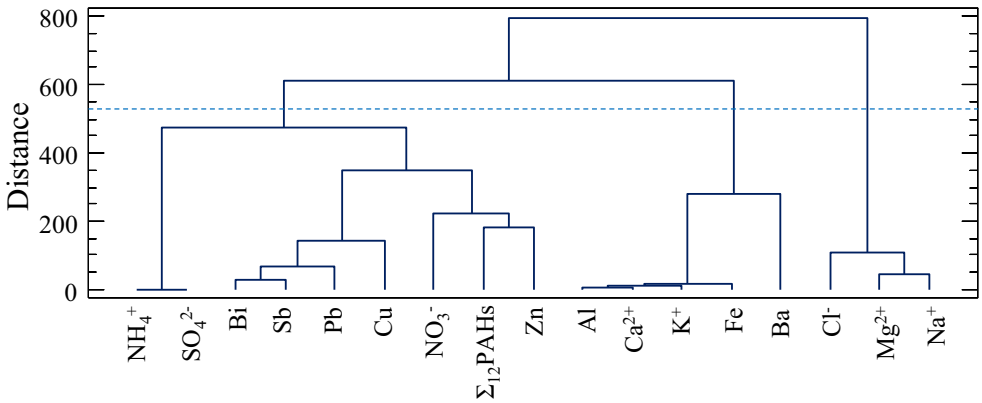

Fig. 6 Dendrogram of the cluster analysis (CA) of major ions, metal(oid)s and Σ_{12}PAH. Σ_{12}PAH = Phe, Ft, Pyr, BaA, Chry, BeP, BbF, BkF, BaP, DBahA, BghiP and IP

Table 3 Lineal model of the variables NO_3^-, Ba, Bi, Cu, Pb, Sb and Zn and PAH concentrations

	Quadratic equations	*p*-value	R^2
Phe	[Phe]=−0.461+0.0068[NO_3^-]+0.125[Ba]+0.115[Bi]+0.039[Cu]+0.217[Pb]+0.096[Sb]−0.025[Zn]	0.0312	0.2270
Ft	[Ft]=−0.625+0.392[NO_3^-]−0.146[Ba]+0.419[Bi]+0.086[Cu]−0.737[Pb]+0.121[Sb]+0.212[Zn]	0.0007	0.3221
Pyr	[Pyr]=−0.553+0.376[NO_3^-]−0.127[Ba]+0.445[Bi]+0.138[Cu]−0.636[Pb]+0.092[Sb]+0.143[Zn]	0.0029	0.2827
BaA	[BaA]=−0.663+0.217[NO_3^-]−0.048[Ba]+0.502[Bi]+0.129[Cu]−0.455[Pb]+0.001[Sb]−0.062[Zn]	0.0132	0.2357
Chry	[Chry]=−0.702+0.306[NO_3^-]−0.091[Ba]+0.588[Bi]+0.058[Cu]−0.784[Pb]−0.053[Sb]−0.227[Zn]	0.0003	0.3439
BeP	[BeP]=−0.445+0.243[NO_3^-]−0.004[Ba]+0.541[Bi]−0.028[Cu]−0.371[Pb]−0.168[Sb]+0.222[Zn]	0.0014	0.3034
BbF	[BbF]=−0.546+0.218[NO_3^-]+0.008[Ba]+0.520[Bi]−0.051[Cu]−0.384[Pb]−0.200[Sb]−0.235[Zn]	0.0016	0.3003
BkF	[BkF]=−0.447+0.292[NO_3^-]−0.022[Ba]+0.596[Bi]+0.0008[Cu]−0.370[Pb]−0.184[Sb]+0.165[Zn]	0.0006	0.3248
BaP	[BaP]=−0.411+0.348[NO_3^-]−0.046[Ba]+0.651[Bi]+0.077[Cu]−0.417[Pb]−0.129[Sb]+0.054[Zn]	0.0006	0.3274
DBahA	[DBahA]=−0.544+0.236[NO_3^-]+0.053[Ba]+0.516[Bi]−0.008[Cu]−0.220[Pb]−0.295[Sb]+0.156[Zn]	0.0011	0.3093
BghiP	[BghiP]=−0.312+0.285[NO_3^-]+0.031[Ba]+0.579[Bi]−0.020[Cu]−0.295[Pb]−0.162[Sb]+0.125[Zn]	0.0006	0.3252
IP	[IP]= −0.242+0.301[NO_3^-]+0.030[Ba]+0.629[Bi]−0.012[Cu]−0.196[Pb]−0.214[Sb]+0.132[Zn]	0.0001	0.3655
Σ_{12}PAHs	[Σ_{12}PAHs]= −0.428+0.296[NO_3^-]−0.015[Ba]+0.605[Bi]+0.006[Cu]−0.454[Pb]−0.144[Sb]+0.192[Zn]	0.0005	0.3339

was found for Σ_{4rings}PAHs with anthropogenic tracer such as Pb (*p* value=0.0220) and Sb (*p* value=0.0282). Similar conclusions were achieved for samples collected during winter and summer seasons.

Principal component and cluster analysis

PCA has been first attempted with a data set in which Phe, Ft, Pyr, BaA, Chry, BeP, BbF, BkF, BaP, DBahA, BghiP and IP concentrations were the discriminating variables and 65 (1-year period), 32 (summer season) and 33 (winter season) PM_{10} samples were the objects. Results (Fig. 4) shown that over 91.45, 96.21 and 91.07% of the variance can be explained by 2 principal components (PCs) for 1-year period, summer and winter season, respectively. The first factor (PC1) was associated with high loadings of high molecular weight PAHs including Chry, BeP, BbF, BkF, BaP, DBahA, BghiP and IP, which were usually abundant in gasoline vehicle emissions and coal combustion (Iakovides et al. 2019). The second factor (PC2) with high loadings of Phe, Ft, Pyr and BaA indicated emissions from diesel vehicles (Teixeira et al. 2015) and coal-biomass combustion (Iakovides et al. 2019). However, high factor loadings were achieved for Pyr in the PC1 during summertime.

PCA has been also attempted with a data set in which ion (Cl^-, NO_3^-, SO_4^{2-}, NH_4^+, K^+, Na^+, Ca^{2+} and Mg^{2+}), metal(oid) (Al, Ba, Bi, Cu, Fe, Sb, Pb and Zn) concentrations and Σ_{12}PAHs were the discriminating variables and 65 (1-year period) PM_{10} samples were the objects. Results show that 72.68% of the total variance was explained by 4 principal

Table 4 $\Sigma_{15}[BaP_{Teq}]$ and $\Sigma_8[BaP_{Meq}]$ concentrations (average ± SD, ng m^{-3}) and Incremental Lifetime Cancer Risk (ILCR) assessment regarding inhalation exposure of the PM_{10}-bound PAH 70-year average life span

	$\Sigma_{15}[BaP_{Teq}]$	$\Sigma_8[BaP_{Meq}]$	WHO ILCR[a]	OEHHA ILCR[b]	USEPA ILCR[c]
Whole period	2.7 ± 3.0	1.4 ± 1.4	$2.4 \times 10^{-4} \pm 2.6 \times 10^{-4}$	$3.0 \times 10^{-6} \pm 3.3 \times 10^{-6}$	$1.6 \times 10^{-6} \pm 1.8 \times 10^{-6}$
Summer season	2.9 ± 3.4	1.4 ± 1.5	$2.5 \times 10^{-4} \pm 3.0 \times 10^{-4}$	$3.2 \times 10^{-6} \pm 3.7 \times 10^{-6}$	$1.8 \times 10^{-6} \pm 2.0 \times 10^{-6}$
Winter season	3.2 ± 2.6	1.7 ± 1.3	$2.7 \times 10^{-4} \pm 2.2 \times 10^{-4}$	$3.5 \times 10^{-6} \pm 2.8 \times 10^{-6}$	$1.9 \times 10^{-6} \pm 1.5 \times 10^{-6}$

[a] ILRC calculated using a $IUR_{BaP} = 8.7 \times 10^{-5}$ $(ng\ m^{-3})^{-1}$ (WHO 2000)

[b] ILRC calculated using a $IUR_{BaP} = 1.1 \times 10^{-6}$ $(ng\ m^{-3})^{-1}$ (OEHHA 2005)

[c] ILRC calculated using a $IUR_{BaP} = 6.0 \times 10^{-7}$ $(ng\ m^{-3})^{-1}$ (USEPA 2017)

components (PCs) which show eigenvalues higher than 1.0 (Fig. 5). K^+, Ba, Ca^{2+}, Mg^{2+}, Al and Fe are the main features in PC1 (crustal/terrestrial source), explaining 36.24% of total variance. The PC2 (vehicle traffic source and fossil fuel combustion) was loaded with Σ_{12}PAHs, NO_3^-, Ba, Bi, Cu, Pb, Sb and Zn (18.04% of the total variance); Pb and Zn are tracers of traffic emission and Cu and Zn could originate from road traffic (Moreda-Piñeiro et al. 2015). PC3 (sea salt source) offers the highest weights for Cl^-, Na^+ and Mg^{2+} (10.59% of the total variance). Also, PC4 is composed of NO_3^-, SO_4^{2-} and NH_4^+ (secondary anthropogenic source) explaining 7.81% of total variance. Finally, cluster analysis (CA) was also performed by using major ion, metal(oid) and Σ_{12}PAH concentrations as variables and 65 (1-year period) PM_{10} samples as objects. CA (Fig. 6) shows that three clusters are formed; the first cluster is formed between Σ_{12}PAHs, NO_3^-, SO_4^{2-} and NH_4^+, Bi, Cu, Pb, Sb and Zn (fuel combustion and vehicle emission source); Al, Ba, Ca^{2+}, Fe and K^+ are the second cluster (crustal source); and the third cluster is formed between Cl^-, Mg^{2+} and Na^+ (marine source). Similar conclusions were achieved after PCA and CA for samples collected during winter and summer seasons.

Multivariate analysis

A multivariate analysis based on linear regression model was performed to test the relationship of major ion and metal(oid) contents and PAH concentrations. As shown in Table 3, predicted PAH concentrations are very close to the measured/observed PAH concentrations (p-value <0.05 for Phe and BaA; and p-values <0.01 for Ft, Pyr, Chry, BeP, BbF, BkF, BaP, DBahA, BghiP, IP and Σ_{12}PAHs) when anthropogenic and traffic road tracers (NO_3^-, Ba, Bi, Cu, Pb, Sb and Zn) were fitted to a quadratic model. The quadratic regression coefficient (R^2) and p-values are also listed in Table 3.

PAH toxicity evaluation

The annual average $\Sigma_{15}[BaP_{Teq}]$ concentration was 2.7 ± 3.0 ng m^{-3}, while the average concentrations during summer and winter seasons were 2.9 ± 3.4 and 3.2 ± 2.6 ng m^{-3}, respectively (Table 4). Concentrations obtained in this study were generally higher than results reported in urban sites of the Southwest Atlantic facade of Europe (Lisbon, 0.185 ± 0.232 ng m^{-3} (Cerqueira and Matos 2019), Oporto, 0.21–3.8 ng m^{-3} (Slezakova et al. 2013a, b) and Santander, 0.11–0.23 ng m^{-3} (Arruti et al. 2012)). Averages of $\Sigma_{16}[BaP_{Teq}]$ concentrations for the warm season were not statistically significant different from that of the cold season ($p > 0.05$). BeP (53–57% of the total $\Sigma_{15}[BaP_{Teq}]$ concentrations) was the major contributor to $\Sigma_{15}[BaP_{Teq}]$ concentrations in both seasons, followed by BaP (14–20%) and DBahA (14–17%), while Phe, Ft, Pyr, Chry and BghiP (< 0.3%) contributed to a lesser extent.

Regarding mutagenic activity, the annual median $\Sigma_8[BaP_{Meq}]$ was 1.4 ± 1.4 ng m^{-3}, although average concentrations were higher during wintertime to those obtained for summer (Table 4). Any seasonal dependence was found for mutagenic activity ($p > 0.05$). BaP and BbF were major contributors of $\Sigma_8[BaP_{Meq}]$ concentrations, accounting for 29–37% (BaP) and 28–35% (BbF). The contribution of IP and BghiP was also important (14–15% and 12–13% for IP and BghiP, respectively).

Estimated $ILCR_{inh}$ values for PM_{10}-bound PAH inhalation exposure (Table 4) show similar values during both seasons. According to the data, average ILCRs exceeded the risk level of 1.0×10^{-4} when using the value of IUR_{BaP} of 8.7×10^{-5} (recommended by WHO (WHO 2000)), suggesting a potentially high risk for human health in the studied area. However, the lung cancer risk was reduced to a potential cancer risk when IUR_{BaP} values of 1.1×10^{-6} (recommended by OEHHA (OEHHA 2005)) and 6.0×10^{-7} (recommended by USEPA (USEPA 2017)) were considered. In addition, it is important to point out that PAH health risk assessment considering ILCRs strongly depends on TEFs, IURs and number of PAHs considered. Then, future efforts focused on the standardization of PAH health risk by using the ILCR approach would be interesting in order to facilitate interpretation and obtain more comparable data.

Conclusions

Sixteen PAH concentrations in PM_{10} collected at a European urban site (Northwest of Spain) mean novel contribution to the knowledge of sources of PAHs in an Atlantic coastal European region. In general, it was found that the concentration of PAHs found at this site was higher than most of other ones reported at Atlantic coast European sites. The average annual concentration of BaP concentration (0.48 ng m^{-3}) did not exceed the target value in PM_{10} set in directive 2004/107/EC. BbF and BeP were the major PAHs found in PM_{10} samples analysed. BghiP, Chry and IP were the next most important contributors. Around 58–60% of the total PAH concentration is attributed to carcinogenic PAHs. Also, PAH concentrations were dominated by higher molecular PAHs (5-ring and 6-ring PAHs recorded around 71–76%). Statistically seasonal differences were not found for all target PAHs. Data from molecular indices and univariate, principal component and cluster analyses suggest a pyrogenic origin (due to the continuous harbour activity and vehicle emissions, which is present throughout the year) of PAHs at urban site during both seasons (summer and winter seasons). Also, statistical multivariate analysis has shown that PAH concentrations are correlated with PM_{10}-bound NO_3^-, Ba, Bi, Cu, Pb, Sb and Zn. Furthermore, PCA suggested that sea salt, anthropogenic and crustal sources were the main PM_{10} formation sources in the studied area. Finally, the health risk assessment based on $ILCR_{inh}$ approach suggested high potential cancer risk for

long-term exposure to PM_{10}-associated PAHs in study area during the sampling period. However, this outcome should be viewed with some caution since it assumes the use of dose response functions based on epidemiology study on coke-oven workers in Pennsylvania and studies on the data from hamsters chronically exposed by inhalation to BaP, but not using data from epidemiology studies associated to PAH inhalation in population from A Coruña city. The present findings are a first step towards a better knowledge of PAH health risk assessment via inhalation in A Coruña city.

Supplementary Information The online version contains supplementary material available at https://doi.org/10.1007/s11869-021-01022-w.

Acknowledgements The council of A Coruña is acknowledged for its assistance (collaboration agreement between the City of A Coruña and the University Institute of Environment (IUMA) of the University of A Coruña (UDC) for the measurement of PM_{10} particle concentrations in the area of Os Castros, A Coruña). The authors would like to thank P. Esperón (PTA2013-8375-I).

Author contribution Idea, P. L.-M. and J. M.-P.; methodology, J. S.-P., M. F.-A. and M. F.-A.; software, J. M.-P.; validation, J. M.-P., M. F.-A. and I. T.-C.; formal analysis, P. L.-M., S. M.-L. and J. M.-P.; investigation, J. M.-P.; resources, P. L.-M., S. M.-L. and J. M.-P.; data curation, J. M.-P., M. F.-A., and J. M.-P.; writing J. M.-P. and J. M.-P..; writing-review and editing J. M.-P. and P. L.-M.; visualization, J. M.-P.; supervision, J. M.-P. and P. L.-M.; project administration, P. L.-M., and S. M.-L.; funding acquisition, P. L.-M., and S. M.-L.

Funding This work was supported by the Ministerio de Ciencia, Innovación y Universidades (MCIU), Agencia Estatal de Investigación (AEI) and Fondo Europeo de Desarrollo Regional (FEDER) (Programa Estatal de I+D+i Orientada a los Retos de la Sociedad, ref: RTI 2018-101116-B-I00), Xunta de Galicia (Programa de Consolidación y Estructuración de Unidades de Investigación Competitivas ref: ED431C 2017/28-2017-2020) and FEDER-MINECO (UNLC15-DE-3097, financed together (80/20%) with Xunta de Galicia). Joel Sánchez-Piñero was supported by the Xunta de Galicia and the European Union (European Social Fund - ESF) for a predoctoral grant (ED481A-2018/164). María Fernández-Amado was supported by the Ministerio de Ciencia, Innovación y Universidades (PTA2017-13607-I).

Data availability Not applicable

Declarations

Ethics approval and consent to participate Not applicable

Consent for publication Not applicable

Conflict of interest The authors declare no competing interests.

References

Abdel-Shafy HI, Mansour MSM (2016) A review on polycyclic aromatic hydrocarbons: Source, environmental impact, effect on human health and remediation. Egypt J Pet 25:107–123. https://doi.org/10.1016/j.ejpe.2015.03.011

Albuquerque M, Coutinho M, Borrego C (2016) Long-term monitoring and seasonal analysis of polycyclic aromatic hydrocarbons (PAHs) measured over a decade in the ambient air of Porto, Portugal. Sci Total Environ 543:439–448. https://doi.org/10.1016/j.scitotenv.2015.11.064

Alves CA, Vicente AMP, Gomes J, Nunes T, Duarte M, Bandowe BAM (2016) Polycyclic aromatic hydrocarbons (PAHs) and their derivatives (oxygenated-PAHs, nitrated-PAHs and azaarenes) in size-fractionated particles emitted in an urban road tunnel. Atmos Res 180:128–137. https://doi.org/10.1016/j.atmosres.2016.05.013

Anderson JO, Thundiyil JG, Stolbach A (2012) Clearing the air: a review of the effects of particulate matter air pollution on human health. J Med Toxicol 8:166–175. https://doi.org/10.1007/s13181-011-0203-1

Arruti A, Fernández-Olmo I, Irabien Á (2012) Evaluation of the urban/rural particle-bound PAH and PCB levels in the northern Spain (Cantabria region). Environ Monit Assess 184:6513–6526. https://doi.org/10.1007/s10661-011-2437-4

Blanco-Heras GA, Turnes-Carou MI, López-Mahía P, Muniategui-Lorenzo S, Prada-Rodríguez D, Fernández-Fernández E (2008) Determination of organic anions in atmospheric aerosol samples by capillary electrophoresis after reversed pre-electrophoresis. Electrophoresis 29:1347–1354. https://doi.org/10.1002/elps.200700413

Brook RD, Rajagopalan S, Pope CA, Brook JR, Bhatnagar A, Diez-Roux AV, Holguin F, Hong Y, Luepker RV, Mittleman MA, Peters A, Siscovick D, Smith SC, Whitsel L, Kaufman JD (2010) Particulate matter air pollution and cardiovascular disease. Circulation 121:2331–2378. https://doi.org/10.1161/CIR.0b013e3181dbece1

Burnett R, Chen H, Szyszkowicz M, Fann N, Hubbell B, Pope CA, Apte JS, Brauer M, Cohen A, Weichenthal S, Coggins J, Di Q, Brunekreef B, Frostad J, Lim SS, Kan H, Walker KD, Thurston GD, Hayes RB, Lim CC, Turner MC, Jerrett M, Krewski D, Gapstur SM, Diver WR, Ostro B, Goldberg D, Crouse DL, Martin RV, Peters P, Pinault L, Tjepkema M, van Donkelaar A, Villeneuve PJ, Miller AB, Yin P, Zhou M, Wang L, Janssen NAH, Marra M, Atkinson RW, Tsang H, Quoc Thach T, Cannon JB, Allen RT, Hart JE, Laden F, Cesaroni G, Forastiere F, Weinmayr G, Jaensch A, Nagel G, Concin H, Spadaro JV (2018) Global estimates of mortality associated with long-term exposure to outdoor fine particulate matter. Proc Natl Acad Sci 201803222:9592–9597. https://doi.org/10.1073/pnas.1803222115

Cao Z, Wang M, Chen Q, Zhu C, Jie J, Li X, Dong X, Miao Z, Shen M, Bu Q (2019) Spatial, seasonal and particle size dependent variations of PAH contamination in indoor dust and the corresponding human health risk. Sci Total Environ 653:423–430. https://doi.org/10.1016/j.scitotenv.2018.10.413

Cerqueira M, Matos J (2019) A one-year record of particle-bound polycyclic aromatic hydrocarbons at an urban background site in Lisbon Metropolitan Area, Portugal. Sci Total Environ 658:34–41. https://doi.org/10.1016/j.scitotenv.2018.12.151

Dat ND, Chang MB (2017) Review on characteristics of PAHs in atmosphere, anthropogenic sources and control technologies. Sci Total Environ 609:682–693. https://doi.org/10.1016/j.scitotenv.2017.07.204

Davy PM, Tremper AH, Nicolosi EMG, Quincey P, Fuller GW (2017) Estimating particulate black carbon concentrations using two offline light absorption methods applied to four types of filter media. Atmos Environ 152:24–33. https://doi.org/10.1016/j.atmosenv.2016.12.010

Draxler RR, Rolph GD (2003) HYSPLIT (HYbrid singleparticle lagrangian integrated trajectory) model access via NOAA ARL READY website. Silver Spring: NOAA Air Resour Lab 96:2059–2077. https://doi.org/10.1175/BAMS-D-14-00110.1

Durant JL, Busby WF, Lafleur AL, Penman BW, Crespi CL (1996) Human cell mutagenicity of oxygenated, nitrated and unsubstituted

polycyclic aromatic hydrocarbons associated with urban aerosols. Mutat Res - Genet Toxicol 371:123–157. https://doi.org/10.1016/S0165-1218(96)90103-2

Elorduy I, Elcoroaristizabal S, Durana N, García JA, Alonso L (2016) Diurnal variation of particle-bound PAHs in an urban area of Spain using TD-GC/MS: influence of meteorological parameters and emission sources. Atmos Environ 138:87–98. https://doi.org/10.1016/j.atmosenv.2016.05.012

EU (2004) Directive 2004/107/EC of the European Parliament and of the Council of 15 December 2004 relating to arsenic, cadmium, mercury, nickel and polycyclic aromatic hydrocarbons in ambient air.

EU (2008) Directive 2008/50/EC of the European Parliament and of the Council of 21 May 2008 on ambient air quality and cleaner air for Europe.

Fernández-Amado M, Prieto-Blanco MC, López-Mahía P, Muniategui-Lorenzo S, Prada-Rodríguez D (2016) A novel and cost-effective method for the determination of fifteen polycyclic aromatic hydrocarbons in low volume rainwater samples. Talanta 155:175–184. https://doi.org/10.1016/J.TALANTA.2016.04.032

Galvão ES, Santos JM, Lima AT, Reis NC, Orlando MTD, Stuetz RM (2018) Trends in analytical techniques applied to particulate matter characterization: a critical review of fundaments and applications. Chemosphere 199:546–568. https://doi.org/10.1016/J.CHEMOSPHERE.2018.02.034

Gao P, Liu D, Guo L, He C, Lin N, Xing Y, Yao C, Wu B, Zheng Z, Wang Y, Hang J (2019) Ingestion bioaccessibility of indoor dust-bound PAHs: inclusion of a sorption sink to simulate passive transfer across the small intestine. Sci Total Environ 659:1546–1554. https://doi.org/10.1016/J.SCITOTENV.2018.12.459

Ghanavati N, Nazarpour A, Watts MJ (2019) Status, source, ecological and health risk assessment of toxic metals and polycyclic aromatic hydrocarbons (PAHs) in street dust of Abadan, Iran. Catena 177:246–259. https://doi.org/10.1016/j.catena.2019.02.022

Gozzi F, Della Ventura G, Marcelli A, Lucci F (2017) Current status of particulate matter pollution in Europe and future perspectives: a review. J Mater Environ Sci 8:1901–1909

Greilinger M, Drinovec L, Močnik G, Kasper-Giebl A (2019) Evaluation of measurements of light transmission for the determination of black carbon on filters from different station types. Atmos Environ 198:1–11. https://doi.org/10.1016/j.atmosenv.2018.10.017

Hoek G, Krishnan RM, Beelen R, Peters A, Ostro B, Brunekreef B, Kaufman JD (2013) Long-term air pollution exposure and cardio-respiratory mortality: a review. Environ Health 12:43. https://doi.org/10.1186/1476-069X-12-43

Iakovides M, Stephanou EG, Apostolaki M, Hadjicharalambous M, Evans JS, Koutrakis P, Achilleos S (2019) Study of the occurrence of airborne Polycyclic aromatic hydrocarbons associated with respirable particles in two coastal cities at Eastern Mediterranean: levels, source apportionment, and potential risk for human health. Atmos Environ 213:170–184. https://doi.org/10.1016/J.ATMOSENV.2019.05.059

IARC (2013) Outdoor air pollution a leading environmental cause of cancer deaths PRESS RELEASE N° 221 17 October 2013. https://www.iarc.who.int/wp-content/uploads/2018/07/pr221_E.pdf (accessed 3.7.21)

Jamhari AA, Sahani M, Latif MT, Chan KM, Tan HS, Khan MF, Mohd Tahir N (2014) Concentration and source identification of polycyclic aromatic hydrocarbons (PAHs) in PM10 of urban, industrial and semi-urban areas in Malaysia. Atmos Environ 86:16–27. https://doi.org/10.1016/j.atmosenv.2013.12.019

Karimi P, Peters KO, Bidad K, Strickland PT (2015) Polycyclic aromatic hydrocarbons and childhood asthma. Eur J Epidemiol 30:91–101. https://doi.org/10.1007/s10654-015-9988-6

Kim KH, Jahan SA, Kabir E, Brown RJC (2013) A review of airborne polycyclic aromatic hydrocarbons (PAHs) and their human health effects. Environ Int 60:71–80. https://doi.org/10.1016/j.envint.2013.07.019

Moreda-Piñeiro J, Turnes-Carou I, Alonso-Rodríguez E, Moscoso-Pérez C, Blanco-Heras G, López-Mahía P, Muniategui-Lorenzo S, Prada-Rodríguez D (2015) The influence of oceanic air masses on concentration of major ions and trace metals in PM2.5 fraction at a coastal European suburban site. Water Air Soil Pollut 226:2240. https://doi.org/10.1007/s11270-014-2240-2

Muñoz X, Barreiro E, Bustamante V, Lopez-Campos JL, González-Barcala FJ, Cruz MJ (2019) Diesel exhausts particles: their role in increasing the incidence of asthma. Reviewing the evidence of a causal link. Sci Total Environ 652:1129–1138. https://doi.org/10.1016/j.scitotenv.2018.10.188

OEHHA (2005) Air Toxics Hot Spots Program Risk Assessment Guidance, Part II - Technical Support document for describing available cancer potency factors. https://oehha.ca.gov/media/downloads/crnr/may2005hotspots.pdf (accessed 3.7.21)

Piñeiro-Iglesias M, López-Mahía P, Muniategui-Lorenzo S, Prada-Rodríguez D, Querol X, Alastuey A (2003) A new method for the simultaneous determination of PAH and metals in samples of atmospheric particulate matter. Atmos Environ 37:4171–4175. https://doi.org/10.1016/S1352-2310(03)00523-5

Piñeiro-Iglesias M, Grueiro-Noche G, López-Mahía P, Muniategui-Lorenzo S, Prada-Rodríguez D (2004) Assessment of methodologies for airborne BaP analysis. Sci Total Environ 334–335:377–384. https://doi.org/10.1016/j.scitotenv.2004.04.041

Quarato M, De Maria L, Gatti MF, Caputi A, Mansi F, Lorusso P, Birtolo F, Vimercati L (2017) Air pollution and public health: a PRISMA-compliant systematic review. Atmosphere (Basel) 8. https://doi.org/10.3390/atmos8100183

Samburova V, Zielinska B, Khlystov A (2017) Do 16 polycyclic aromatic hydrocarbons represent PAH air toxicity? Toxics 5:17. https://doi.org/10.3390/toxics5030017

Simonetti G, Conte E, Massimi L, Frasca D, Perrino C, Canepari S (2018) Oxidative potential of particulate matter components generated by specific emission sources. J Aerosol Sci 126:99–109. https://doi.org/10.1016/j.jaerosci.2018.08.011

Slezakova K, Castro D, Delerue-Matos C, Alvim-Ferraz M d C, Morais S, Pereira M d C (2013a) Impact of vehicular traffic emissions on particulate-bound PAHs: levels and associated health risks. Atmos Res 127:141–147. https://doi.org/10.1016/j.atmosres.2012.06.009

Slezakova K, Pires JCM, Castro D, Alvim-Ferraz MCM, Delerue-Matos C, Morais S, Pereira MC (2013b) PAH air pollution at a Portuguese urban area: carcinogenic risks and sources identification. Environ Sci Pollut Res 20:3932–3945. https://doi.org/10.1007/s11356-012-1300-7

Taioli E, Sram RJ, Garte S, Kalina I, Popov TA, Farmer PB (2007) Effects of polycyclic aromatic hydrocarbons (PAHs) in environmental pollution on exogenous and oxidative DNA damage (EXPAH project): description of the population under study. Mutat Res Mol Mech Mutagen 620:1–6. https://doi.org/10.1016/J.MRFMMM.2007.02.016

Teixeira EC, Agudelo-Castañeda DM, Fachel JMG, Leal KA, Garcia K d O, Wiegand F (2012) Source identification and seasonal variation of polycyclic aromatic hydrocarbons associated with atmospheric fine and coarse particles in the Metropolitan Area of Porto Alegre, RS, Brazil. Atmos Res 118:390–403. https://doi.org/10.1016/j.atmosres.2012.07.004

Teixeira EC, Agudelo-Castañeda DM, Mattiuzi CDP (2015) Contribution of polycyclic aromatic hydrocarbon (PAH) sources to the urban environment: a comparison of receptor models. Sci Total Environ 538:212–219. https://doi.org/10.1016/j.scitotenv.2015.07.072

Tobías A, Rivas I, Reche C, Alastuey A, Rodríguez S, Fernández-Camacho R, Sánchez de la Campa AM, de la Rosa J, Sunyer J, Querol X (2018) Short-term effects of ultrafine particles on daily

mortality by primary vehicle exhaust versus secondary origin in three Spanish cities. Environ Int 111:144–151. https://doi.org/10.1016/j.envint.2017.11.015

UNE (2015) UNE-EN 12341:2015. Air Quality - Determination of the PM10 fraction of suspended particulate matter - reference method and field test procedure to demonstrate reference equivalence of measurement methods [WWW Document]. URL https://www.une.org/encuentra-tu-norma/busca-tu-norma/norma?c=N0054246 (accessed 7.23.19)

USEPA (1984) Method 610: polynuclear aromatic hydrocarbons. URL https://www.epa.gov/sites/production/files/2015-10/documents/method_610_1984.pdf (accessed 3.7.21)

USEPA (2005) Human health risk assessment protocol for hazardous waste combustion facilities. US Environmental Protection Agency. Washington, DC. URL https://archive.epa.gov/epawaste/hazard/tsd/td/web/pdf/05hhrapcover.pdf (accessed 3.7.21)

USEPA (2011) Integrated Risk Information System (IRIS) Glossary. URL https://www.epa.gov/iris (accessed 3.7.21)

USEPA (2017) Toxicological review of benzo[a]pyrene - integrated risk information system. URL https://cfpub.epa.gov/ncea/iris_drafts/recordisplay.cfm?deid=329750 (accessed 3.7.21).

Vicente ED, Vicente A, Evtyugina M, Carvalho R, Tarelho LAC, Oduber FI, Alves C (2018) Particulate and gaseous emissions from charcoal combustion in barbecue grills. Fuel Process Technol 176:296–306. https://doi.org/10.1016/j.fuproc.2018.03.004

Wang W, Huang, Juan M, Kang Y, Wang, Sheng H, Leung AOW, Cheung KC, Wong MH (2011) Polycyclic aromatic hydrocarbons (PAHs) in urban surface dust of Guangzhou, China: status, sources and human health risk assessment. Sci. Total Environ 409:4519–4527. https://doi.org/10.1016/j.scitotenv.2011.07.030

WHO (2000) Air Quality Guidelines for Europe (Second Edition). URL https://www.euro.who.int/en/health-topics/environment-and-health/air-quality/publications/pre2009/who-air-quality-guidelines-for-europe,-2nd-edition,-2000-cd-rom-version (accessed 3.7.21)

WHO (2010) WHO guidelines for indoor air quality: selected pollutants. URL https://www.euro.who.int/__data/assets/pdf_file/0009/128169/e94535.pdf (accessed 3.7.21)

Yunker MB, Macdonald RW, Vingarzan R, Mitchell RH, Goyette D, Sylvestre S (2002) PAHs in the Fraser River basin: a critical appraisal of PAH ratios as indicators of PAH source and composition. Org Geochem 33:489–515. https://doi.org/10.1016/S0146-6380(02)00002-5